*Inorg. Chem.* **2005**, *44*, 9862–9873


# Tetra-2,3-pyrazinoporphyrazines with Externally Appended Pyridine Rings. 4. UV–Visible Spectral and Electrochemical Evidence of the Remarkable Electron-Deficient Properties of the New Tetrakis-2,3-[5,6-di{2-(*N*-methyl)pyridiniumyl}pyrazino]porphyrazinatometal Octacations, $[(2\text{-Mepy})_8\text{TPyzPzM}]^{8+}$ (M = $Mg^{II}(H_2O)$, $Co^{II}$, $Cu^{II}$, $Zn^{II}$)

**Costanza Bergami,[§] Maria Pia Donzello,[§] Fabrizio Monacelli,[§] Claudio Ercolani,*[,§] and Karl M. Kadish*[,#]**

*Dipartimento di Chimica, Università degli Studi di Roma "La Sapienza", p.le A. Moro 5, I-00185 Roma, Italy, and Department of Chemistry, University of Houston, Houston, Texas 77204-5003*

Received June 30, 2005

Metal derivatives of the octacationic tetrakis-2,3-[5,6-di{2-(*N*-methyl)pyridiniumyl}pyrazino]porphyrazine macrocycle $[(2\text{-Mepy})_8\text{TPyzPzH}_2]^{8+}$ (2-Mepy = 2-(*N*-methyl)pyridiniumyl ring) isolated as water-soluble hydrated iodide salts of the general formula $[(2\text{-Mepy})_8\text{TPyzPzM}](I_8)\cdot x H_2O$, (M = $Mg^{II}(H_2O)$, $Co^{II}$, $Cu^{II}$, $Zn^{II}$; $x$ = 2–5) were prepared from the corresponding neutral complexes $[Py_8\text{TPyzPzM}]\cdot x H_2O$ previously reported. Reaction of these complexes with $CH_3I$ in *N,N*-dimethylformamide under mild conditions led to full quaternization of all eight pyridine N atoms and formation of the octacations $[(2\text{-Mepy})_8\text{TPyzPzM}]^{8+}$. Clathrated water molecules could be eliminated from the species $[(2\text{-Mepy})_8\text{TPyzPzM}](I_8)\cdot x H_2O$ by mild heating ($\leq$100 °C) under vacuum, but the unsolvated species which were formed tended to rehydrate when exposed to air. Magnetic susceptibility measurements and EPR spectra prove that the $Cu^{II}$ and $Co^{II}$ complexes in the solid state are both paramagnetic with one unpaired electron, thus giving a low-spin state $Co^{II}$ for the latter compound. Studies of the charged species $[(2\text{-Mepy})_8\text{TPyzPzM}]^{8+}$ in aqueous media at ca. $10^{-5}$ M concentration provide evidence for the occurrence of molecular aggregation, similar to what is seen for the related free-base species $[(2\text{-Mepy})_8\text{TPyzPzH}_2]^{8+}$ (see part 3 of this series, preceding paper in this issue), but the formation of monomeric species is generally favored upon dilution of the solutions. The same octacations are essentially monomeric in solutions of pyridine or dimethyl sulfoxide (DMSO), but traces of aggregation, if occasionally present, vanish with the time. Changes in the UV–visible spectra are observed in the Q- and B-band regions as a result of the quaternization at the pyridine N atoms. Cyclic voltammetry and thin-layer spectroelectrochemical data in DMSO show well-resolved reversible multistep one-electron reductions for both the unmethylated and methylated complexes, all of which appear to be ligand-centered, the only exception being reduction of the $Co^{II}$ complex. For this species, the first one-electron reduction is a metal-centered $Co^{II} \rightarrow Co^{I}$ process, but the site of electron transfer is reversed and the final product upon a further one-electron reduction is formulated as a $Co^{II}$ dianion as opposed to a $Co^{I}$ $\pi$-anion radical. This sequence is similar to what was earlier reported for reduction of the same compound in pyridine. Reversible one-electron oxidations are also observed for the unmethylated species $[Py_8\text{TPyzPzM}]\cdot x H_2O$ where M = $Co^{II}$ and $Mn^{II}$ in DMSO. Remarkably, the octacationic macrocycles $[(2\text{-Mepy})_8\text{TPyzPzM}](I_8)\cdot x H_2O$, (M = $Mg^{II}(H_2O)$, $Co^{II}$, $Cu^{II}$, and $Zn^{II}$; $x$ = 2–5) are more easily reduced at any step of the reduction than the corresponding unquaternized species with the same metal ion. This indicates a higher tendency to stepwise electron uptake after the quaternization process, which enhances the charge redistribution capability within the species formed by the electroreduction.

## Introduction

In recent years the synthesis and characterization of new porphyrazine macrocycles carrying strongly electron withdrawing heterocyclic rings annulated at the peripheral sites of the central porphyrazine core has attracted our interest (see ref 5 in the previous companion paper to this work[1]). A

* To whom correspondence should be addressed. E-mail: claudio.ercolani@uniroma1.it (C.E.), kkadish@uh.edu (K.M.K.).

[§] Università degli Studi di Roma "La Sapienza".
[#] University of Houston.



10.1021/ic051085d CCC: $30.25 
Published on Web 11/19/2005

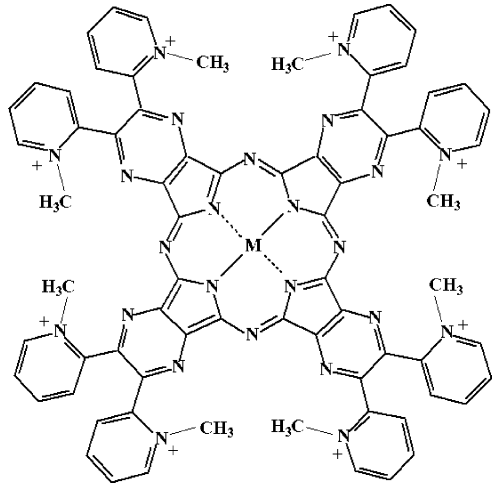

**Figure 1.** Schematic representation of $[(2\text{-Mepy})_8\text{TPyzPzM}]^{8+}$ (M = $Mg^{II}(H_2O)$, $Co^{II}$, $Cu^{II}$, or $Zn^{II}$).

new tetrapyrazinoporphyrazine carrying externally appended pyridine rings, i.e., tetrakis-2,3-[5,6-di(2-pyridyl)pyrazino]-porphyrazine, $[Py_8TPyzPzH_2]$, was also recently reported.[2] It was shown that the four external dipyridinopyrazine fragments significantly enhance the overall electron-deficient properties of the entire macrocycle through $\sigma$ and $\pi$ bond mechanisms of charge transmission, with relevant effects on the acidity strength of the macrocycle. Along the same lines, electrochemical measurements on the unmetalated macrocycle,[2] $[Py_8TPyzPzH_2]$, and a number of its metal derivatives, $[Py_8TPyzPzM]$ (M = $Mg^{II}(H_2O)$, $Mn^{II}$, $Co^{II}$, $Cu^{II}$, $Zn^{II}$), have shown[3] that the "octapyridinotetrapyrazinoporphyrazine" macrocycle manifests a marked tendency toward stepwise electron capture, which is remarkably more facile than for the parallel series of phthalocyanine and porphyrin analogues.

A previous companion paper in this series[1] reports the synthesis and characterization of the octacationic water-soluble unmetalated macrocycle tetrakis-2,3-[5,6-di{2-(*N*-methyl)pyridiniumyl}pyrazino]porphyrazine, $[(2\text{-Mepy})_8\text{TPyzPzH}_2]^{8+}$, neutralized by $I^-$ ions and obtained as a hydrated species of the formula $[(2\text{-Mepy})_8\text{TPyzPzH}_2](I_8)\cdot 8H_2O$ (2-Mepy = 2(*N*-methyl)pyridiniumyl moiety) by demetalation of its corresponding $Mg^{II}$ complex, $[(2\text{-Mepy})_8\text{TPyzPzMg}(H_2O)](I_8)\cdot 5H_2O$.

This current contribution extends our studies to include metal complexes of this macrocycle having the general formula $[(2\text{-Mepy})_8\text{TPyzPzM}](I)_8\cdot x(H_2O)$ ($x$ = 2−5), M being $Mg^{II}(H_2O)$ or a first-row transition-metal ion ($Co^{II}$, $Cu^{II}$, or $Zn^{II}$) (Figure 1). This series of metal complexes has been characterized by IR, UV−visible, and EPR spectroscopy, magnetic susceptibility, electrochemistry, and spectroelectrochemistry. One main target of this work was to examine changes in the electronic distribution which is produced on the macrocyclic unit by quaternization at the N atoms of the externally appended pyridine rings and to measure the resulting effects by monitoring the UV−visible spectra and redox behavior of these compounds.

## Experimental Section

Solvents and reagents were used as received, unless otherwise specified. The hydrated free-base macrocycle $[Py_8TPyzPzH_2]\cdot 2H_2O$, was obtained as reported in part 1 of this series.[2] Either dimethyl sulfoxide (DMSO), freshly distilled over $CaH_2$, or pyridine was used for synthesis of the hydrated complexes having the general formula $[Py_8TPyzPzM]\cdot xH_2O$ (M = $Mg^{II}(H_2O)$, $Mn^{II}$, $Co^{II}$, $Cu^{II}$, and $Zn^{II}$).[3] When obtained from pyridine, the complexes were heated under vacuum at 150 °C before use. Synthesis of the $Mg^{II}$ complex monoaquotetrakis-2,3-[5,6-di{2-(*N*-methyl)pyridiniumyl}pyrazino]-porphyrazinatomagnesium(II) octaiodide pentahydrate, $[(2\text{-Mepy})_8\text{-TPyzPzMg}(H_2O)](I)_8\cdot 5H_2O$, was accomplished as described in an accompanying paper.[1]

**Tetrakis-2,3-[5,6-di{2-(*N*-methyl)pyridiniumyl}pyrazino]-porphyrazinatocobalt(II) Octaiodide Trishydrate, $[(2\text{-Mepy})_8\text{-TPyzPzCo}](I)_8\cdot 3H_2O$.** The complex $[Py_8TPyzPzCo]\cdot 6H_2O$ (103 mg, 0.078 mmol) and $CH_3I$ (2 mL, 32.13 mmol) were added to dimethylformamide (DMF, 4 mL), and the mixture was heated at 50 °C for 48 h. After evaporation of $CH_3I$ in air at room temperature, the mixture was kept in the refrigerator for 2 days. After centrifugation, the dark green solid which separated was washed with benzene and ether and then brought to constant weight under vacuum (184 mg, yield 99%). Calcd for $[(2\text{-Mepy})_8\text{TPyzPzCo}](I_8)\cdot 3H_2O$, $C_{72}H_{62}CoI_8N_{24}O_3$: C, 36.25; H, 2.62; N, 14.09. Found C, 36.33; H, 2.57; N, 14.70%. IR ($cm^{-1}$) (KBr): 3540 broad m, 1622 w, 1579 w, 1559 w, 1520 w, 1498 vw, 1485 vw, 1461 vw, 1408 vw, 1384 vw, 1356 w, 1336 m, 1281 vw, 1247 m, 1187 wm, 1153 w, 1125 vw, 1096 w, 999 w, 973 w, 950 w, 824 vw, 778 broad wm, 750 wm, 716 w, 707 wm, 661 w, 622 vw, 605 vw, 586 vw, 568 vw, 512 vvw, 443 wm, 415 w. Thermogravimetric analysis shows a 2.5% weight loss (water) from room temperature up to 100 °C (calcd for $3H_2O$: 2.26%).

**Tetrakis-2,3-[5,6-di{2-(*N*-methyl)pyridiniumyl}pyrazino]-porphyrazinatocopper(II) Octaiodide Tetrahydrate, $[(2\text{-Mepy})_8\text{TPyzPzCu}](I)_8\cdot 4H_2O$.** The complex $[Py_8TPyzPzCu]\cdot 5H_2O$ (114 mg, 0.088 mmol) and $CH_3I$ (1.2 mL, 19.3 mmol) were added to DMF (2.5 mL), and the mixture was heated at 50 °C for 48 h. After evaporation of $CH_3I$ in air at room temperature, a precipitate was separated first, washed with benzene and ether, and then dried (32.3 mg). Benzene (5 mL) was then added, and the solution was kept in the refrigerator for 2 days. Additional solid, which separated, was washed with benzene and ether and brought to constant weight under vacuum (69.1 mg, yield 33%). Calcd for $[(2\text{-Mepy})_8\text{TPyzPzCu}](I)_8\cdot 4H_2O$, $C_{72}H_{64}CuI_8N_{24}O_4$: C, 35.91; H, 2.68; N, 13.96. Found C, 35.41; H, 3.00; N, 13.15%. IR ($cm^{-1}$) (KBr): 3047 broad w, 3009 w, 1625 s, 1582 ms, 1556 m, 1511 ms, 1484 m, 1456 m, 1436 vw, 1428 vw, 1404 w, 1388 w, 1363 ms, 1281 w, 1252 vs, 1197 wm, 1184 wm, 1176 sh, 1148 w, 1120 s, 1096 w, 1044 w, 1020 w, 997 m, 963 ms, 946 ms, 936 vw, 918 vw, 866 vw, 829 w, 806 vvw, 781 m, 749 m, 717 m, 703 s, 659 m, 628 w, 620 w, 602 vw, 568 wm, 537 vw, 510 vw, 442 wm. Thermogravimetric analysis shows a 2.67% weight loss (water) from room temperature up 100 °C (calcd for 4 $H_2O$: 2.99%).


(1) Part 3: Bergami, C.; Donzello, M. P.; Ercolani, C.; Monacelli, F.; Kadish, K. M.; Rizzoli, C. *Inorg. Chem.* **2005**, *44*, 9852−9861.

(2) Donzello, M. P.; Ou, Z.; Monacelli, F.; Ricciardi, G.; Rizzoli, C.; Ercolani, C.; Kadish, K. M. *Inorg. Chem.* **2004**, *43*, 8626.

(3) Donzello, M. P.; Ou, Z.; Dini, D.; Meneghetti, M.; Ercolani, C.; Kadish, K. M. *Inorg. Chem.* **2004**, *43*, 8637.

(4) (a) Stuzhin, P. A.; Ercolani, C. In *The Porphyrin Handbook*; Kadish, K. M., Smith, K. M., Guilard, R., Eds.; Academic Press: New York, 2003; Vol. 15, Chapter 101, pp 263−364. (b) Kudrevich, S. V.; van Lier, J. E. *Coord. Chem. Rev.* **1996**, *156*, 163.

(5) Figgis, B. M.; Lewis, J. In *Modern Coordination Chemistry*; Lewis, J., Wilkins, R. G., Eds.; Interscience Publishers Inc.: New York, 1960; pp 400−454.

**Table 1.** Room Temperature Magnetic Moments and EPR Data of $[(2\text{-Mepy})_8\text{TPyzPzM}](I_8)\cdot x H_2O$ Complexes (M = $Cu^{II}$, $Co^{II}$)

| complex[a] | $\mu_{eff}$[c] ($\mu_B$) | $g_{\|}$ | $g_{\perp}$ | $A_{\|}^M$ (G) | $A_{\perp}^M$ (G) | $A_{\|}^N$ (G) | ref |
|---|---|---|---|---|---|---|---|
| $[Py_8\text{TPyzPzCu}]\cdot 5H_2O$[b] | 1.91 | 2.173 | 2.056 | 2.05 | 16 | 16 | 3 |
| $[(2\text{-Mepy})_8\text{TPyzPzCu}](I_8)\cdot 2H_2O$[b] | 1.95 | 2.171 | 2.053 | 2.05 | 17 | 15 | tw[d] |
| $[(2\text{-Mepy})_8\text{TPyzPzCo}](I_8)\cdot 2H_2O$[b] | 2.28 | | | | | | tw[d] |

[a] Water molecules are given as fixed by elemental analysis and TGA for the particular sample used for the measurements. [b] Samples prepared by magnetic dilution in the corresponding $Zn^{II}$ complex matrix; no data reported for the $Co^{II}$ complex due to the poor EPR spectrum obtained. [c] $\mu_{eff} = 2.84 \times (\chi_M' \times T)^{1/2}$. [d] tw = this work.

**Tetrakis-2,3-[5,6-di{2-(*N*-methyl)pyridiniumyl}pyrazino]porphyrazinatozinc(II) Octaiodide Dihydrate, $[(2\text{-Mepy})_8\text{TPyzPzZn}](I)_8\cdot 2H_2O$.** The complex $[Py_8\text{TPyzPzZn}]\cdot 3H_2O$ (99.6 mg, 0.079 mmol) and $CH_3I$ (0.8 mL, 12.85 mmol) were added to DMF (1.6 mL), and the mixture was heated at 50 °C for 48 h. After evaporation of $CH_3I$ in air at room temperature, a precipitate was separated first, washed with benzene and ether, and then dried (19.7 mg). Benzene (5 mL) was then added, and the solution was kept in the refrigerator for 2 days. More dark green solid which separated was washed with benzene and ether and brought to constant weight under vacuum (112.8 mg, yield 60%). Calcd for $[(2\text{-Mepy})_8\text{TPyzPzZn}](I)_8\cdot 2H_2O$, $C_{72}H_{60}CuI_8N_{24}O_2Zn$: C, 36.43; H, 2.55; N, 14.16. Found C, 35.61; H, 3.30; N, 13.71%. IR ($cm^{-1}$) (KBr): 3022 broad wm, 2754 w, 2393 wm, 2285 w, 1790 vw, 1750 w, 1732 w, 1673 wm, 1627 s, 1582 ms, 1547 wm, 1511 wm, 1491 wm, 1460 m, 1454 wm, 1439 w, 1400 w, 1362 ms, 1285 w, 1247 s, 1180 m, 1150 w, 1112 m, 1090 w, 1051 w, 997 m, 955 m, 884 w, 845 w, 828 w, 778 m, 743 m, 700 s, 692 w, 655 m, 627 wm, 605 w, 569 wm, 523 w, 509 w, 440 m. Thermogravimetric analysis shows a 1.84% weight loss (water) from room temperature up to 100 °C (calcd for 2 $H_2O$: 1.52%).

**Electrochemical and Spectroelectrochemical Measurements.** Cyclic voltammetric (CV) measurements were performed at room temperature on an EG&G model 173 potentiostat coupled with an EG&E model 175 universal programmer in DMSO (Aldrich, anhydrous, 99.8%) solution containing 0.1 M tetrabutylammonium perchlorate (TBAP) as supporting electrolyte. High purity $N_2$ from Trigas was used to deoxygenate the solution before each electrochemical experiment. TBAP was purchased from Sigma Chemical or Fluka Chemika Co., recrystallized from ethyl alcohol, and dried under vacuum at 40 °C for at least 1 week prior to use. A three electrode system was used and consisted of a glassy carbon working electrode, a platinum wire counter electrode, and a saturated calomel reference electrode (SCE). The reference electrode was separated from the bulk solution by a fritted-glass bridge filled with the solvent, supporting electrolyte mixture. Thin-layer spectroelectrochemistry measurements were carried out at optically transparent thin-layer Pt working electrode using a Hewlett-Packard Model 8453 diode array spectrophotometer coupled with an EG&G Model 173 universal programmer. These measurements were carried out in solutions containing 0.2 M TBAP as supporting electrolyte.

**Other Physical Measurements.** IR spectra were taken with a Perkin-Elmer 1760 X spectrophotometer in the range 4000−400 $cm^{-1}$ by using KBr pellets. UV−visible solution spectra other than those for spectroelectrochemistry (see above) were recorded with a Varian Cary 5E spectrometer. Thermogravimetric analyses (TGA) were performed on a Stanton Redcroft Model STA-781 analyzer under a $N_2$ atmosphere (0.5 L/min). Elemental analyses for C, H, and N were provided by the "Servizio di Microanalisi" at the Dipartimento di Chimica, Università "La Sapienza" (Rome) on an EA 1110 CHNS-O instrument. Room-temperature magnetic susceptibility measurements were carried out by the Gouy method using a $NiCl_2$ solution as calibrant. EPR spectra at room temperature were recorded on a Varian V 4502-4 spectrometer, at the Dipartimento di Chimica, Università "La Sapienza" (Rome).

## Results and Discussion

**Preparative Aspects and Solid State Properties.** Metal derivatives of the fully quaternized porphyrazine macrocycle $[(2\text{-Mepy})_8\text{TPyzPzH}_2]^{8+}$ were obtained in fairly good yields as hydrated iodide salts having the formula $[(2\text{-Mepy})_8\text{TPyzPzM}](I_8)\cdot x(H_2O)$ (M = $Mg^{II}(H_2O)$, $Co^{II}$, $Cu^{II}$, or $Zn^{II}$; $x = 2-5$). This was accomplished by methylation at the pyridine N atoms of the corresponding neutral $[Py_8\text{TPyzPzM}]\cdot x H_2O$ by using $CH_3I$ in DMF. As was the case for the free-base macrocycle,[1] unsatisfactory results were obtained by using methyl *p*-toluenesulfonate as the methylating agent since mixtures of partially quaternized materials were invariably obtained.

The systematic presence of clathrated water molecules (hereafter neglected in the formulas given, unless specifically required) is a common feature for macrocycles carrying externally annulated heterocyclic rings, as has been frequently pointed out.[1,4] This is also observed in the present study and, although the number of water molecules is specified for each complex in the Experimental Section, it was verified that the actual water content found could vary significantly for different samples of the same metal complex. Thermogravimetric analysis shows that all of the metal complexes, once desolvated, are stable in an inert atmosphere up to ca. 200 °C or slightly above. Exposure of the heated samples to air leads to rehydration of the materials. The $Mg^{II}$ cationic fragment is formulated with one water molecule directly ligated to the metal, i.e., $[(2\text{-Mepy})_8\text{TPyzPzMg}(H_2O)]^{8+}$. The aspect of water coordination to $Mg^{II}$ and/or water association was discussed in part 2 of this series[3] and is not further considered in the present manuscript.

Room-temperature magnetic susceptibility was measured for the $Mg^{II}$, $Zn^{II}$, $Co^{II}$, and $Cu^{II}$ complexes. The EPR spectrum of the $Cu^{II}$ complex, magnetically diluted in the corresponding $Zn^{II}$ analogue, was also measured. The values of the molar susceptibility $\chi_M'$ measured directly for the diamagnetic $Mg^{II}$ and $Zn^{II}$ species are, respectively, $-1126 \times 10^{-6}$ and $-1182 \times 10^{-6}$ cgsu, in fairly good agreement with values calculated by the Pascal constants, i.e., $1116 \times 10^{-6}$ and $1126 \times 10^{-6}$ cgsu.[5] The experimental value of the $Mg^{II}$ complex was taken as the diamagnetic contribution for the calculation of the magnetic moments of the $Cu^{II}$ and $Co^{II}$ complexes, after appropriate corrections for the different metal centers and number of associated water molecules. As shown in Table 1, the $\mu_{eff}$ values for the two metal complexes are consistent with the presence of one unpaired electron,

**Table 2.** UV−Visible Spectral Data for the Hydrated Species [(2-Mepy)$_8$TPyzPzM](I$_8$)[a] and the Related Unquaternized Analogues [Py$_8$TPyzPzM][b] in Different Solvents

| | | $\lambda$ [nm] (log $\epsilon$) | | | | | | |
|---|---|---|---|---|---|---|---|---|
| metal complex | solvent | Soret region | | Q-band region | | | | ref |
| [Mg$^{II}$] | py | 375 (5.23) | | | 596 (4.65) | 631 (sh) (4.64) | 658 (5.54) | 3 |
| | DMSO | 374 (5.08) | | 566 (sh) (3.96) | 594 (4.36) | 629 (sh) (4.55) | 653 (5.34) | tw |
| [Mg$^{II}$]$^{8+}$ | py | 368 (4.06) | 410 (sh) (3.81) | 578 (sh) (3.22) | 605 (3.59) | 642 (sh) (3.66) | 673 (4.34) | tw |
| | DMSO | 370 (4.83) | 415 (sh) (4.56) | 562 (sh) (3.80) | 600 (4.33) | 630 (sh) (4.33) | 660 (5.15) | tw |
| | H$_2$O ($1.26 \times 10^{-7}$ M) | 366 (5.71) | | 601 (5.18) | | 631 (sh) (5.35) | 657 (5.94) | tw |
| [Zn$^{II}$] | py | 378 (4.90) | | 598 (4.31) | | 630 (sh) (4.35) | 658 (5.18) | 3 |
| | DMSO | 372 (5.10) | | 565 (sh) (4.02) | 592 (4.54) | 629 (sh) (4.61) | 655 (5.36) | tw |
| [Zn$^{II}$]$^{8+}$ | py | 373 (4.92) | 468 (sh) (4.09) | | 607 (4.38) | 640 (sh) (4.48) | 673 (5.23) | tw |
| | DMSO | 373 (4.37) | | | 600 (sh) (3.86) | 637 (sh) (3.89) | 666 (4.74) | tw |
| | H$_2$O ($5.18 \times 10^{-7}$ M) | 360 (4.89) | | | | 626 (4.69) | 654 (4.70) | tw |
| [Cu$^{II}$] | py | 379 (4.64) | | | 591 (4.18) | | 653 (4.93) | 3 |
| | DMSO | 365 (4.91) | | | 590 (4.44) | | 648 (5.18) | tw |
| [Cu$^{II}$]$^{8+}$ | py | 372 (4.98) | | | | 612 (sh) (4.64) | 662 (5.00) | tw |
| | DMSO | 359 (4.95) | | 560 (sh) (4.07) | 593 (4.46) | | 655 (5.18) | tw |
| | H$_2$O ($1.01 \times 10^{-7}$ M) | 362 (4.77) | | | 596 (sh) (4.24) | | 655 (4.82) | tw |
| [Co$^{II}$] | py | 364 (5.01) | 441 (4.40) | | 575 (sh) (4.38) | | 635 (4.94) | 3 |
| | DMSO | 355 (5.23) | 45 (sh) (4.65) | | 586 (sh) (4.71) | | 634 (5.24) | tw |
| [Co$^{II}$]$^{8+}$ | py | 364 (5.09) | 471 (sh) (4.59) | | 589 (4.55) | | 656 (5.03) | tw |
| | DMSO | 360 (5.02) | 462 (sh) (4.36) | | 583 (sh) (4.35) | | 642 (4.97) | tw |
| | H$_2$O | 354 (4.95) | 445 (4.33) | | 590 (4.34) | | 645 (4.89) | tw |

[a] Abbreviated in the table as [M$^{II}$]$^{8+}$. [b] Abbreviated in the table as [M$^{II}$].

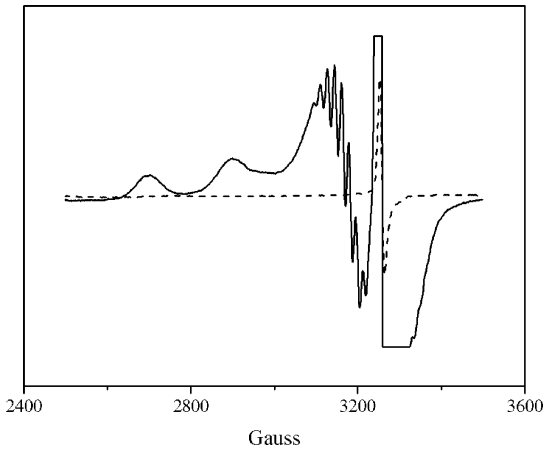


**Figure 2.** Room-temperature EPR spectra of hydrated [(2-Mepy)$_8$TPyzPzCu](I$_8$) magnetically diluted in its corresponding Zn$^{II}$ matrix (solid line) and of [(2-Mepy)$_8$TPyzPzZn](I$_8$) (dashed line). The sharp signal present just above 3200 G in both materials is due to an impurity present in the Zn$^{II}$ complex.

as expected for Cu$^{II}$ (d$^9$) and Co$^{II}$ complexes (d$^7$), the latter being in a low-spin state. These results are in line with previous findings for the corresponding unquaternized species[3] and related tetrapyrrolic analogues.[3,6−8] Table 1 gives the EPR spectral data of the Cu$^{II}$ complex, which shows hyperfine and superhyperfine structure (Figure 2) indicating delocalization of the unpaired electron within the CuN$_4$ central chromophore. Values of the measured parameters are very similar to those of the corresponding unquaternized Cu$^{II}$ analogue.[3]

**Solution UV−Visible Spectral Studies in Water, Pyridine, and DMSO of the Cations [(2-Mepy)$_8$TPyzPzM]$^{8+}$. (a) Water.** The Mg$^{II}$, Cu$^{II}$, and Zn$^{II}$ complexes show similar spectra in water solution with two maxima of comparable intensity appearing in the Q-band region (at ca. 620−630 and ca. 655 nm) and a B band at 360−366 nm (Table 2). The spectra at $c \cong 10^{-5}$ M do not change significantly as a function of time (hours). However, when the solutions are examined as a function of decreasing concentration from $10^{-4}$ to $10^{-7}$ M, changes occur in the Q-band region which lead, for all three complexes, to an increase in intensity of the band at ca. 655 nm and a decrease in absorbance for the band at ca. 620−630 nm. For the Mg$^{II}$ and Cu$^{II}$ complexes, at $10^{-7}$ M concentration (Figure 3A,B), the band at 620−630 nm has completely disappeared, and only the narrow Q band at ca. 655 nm is seen; thus the spectra conform to that expected for the monomeric form of the compounds ($D_{4h}$ symmetry, unsplit Q band[9]). This spectral behavior indicates that the band at ca. 620−629 nm belongs to an aggregated species (probably a dimer) which disaggregates upon dilution. Although the tendency of the Zn$^{II}$ derivative to disaggregate is also shown, it is observed that at $10^{-7}$ M concentration, the monomeric form is not exclusively present, i.e., some aggregate species is still present in solution (Figure 3C).

The spectrum of the Co$^{II}$ species in water shows an unsplit Q band at 645 nm with a vibrational component on the blue side, a symmetrical B band at 354 nm, and a low-intensity absorption at ca. 445 nm. The spectrum (not shown) undergoes slow subtle changes with time, plausibly because of disappearing residual traces of aggregation, not necessarily of the type evidenced for the Mg$^{II}$, Cu$^{II}$, and Zn$^{II}$ complexes. The Q and B bands reach their maximum stable intensity after a few hours, which allows calculation of the $\epsilon$ values for the monomeric form of the compound (Table 2). From these and the above data for the Mg$^{II}$, Cu$^{II}$, and Zn$^{II}$ complexes, it can be concluded that molecular aggrega-

(6) Donzello, M. P.; Dini, D.; D'Arcangelo, G.; Ercolani, C.; Kadish, K. M.; Ou, Z.; Stuzhin, P. A.; Zhan, R. *J. Am. Chem. Soc.* **2003**, *125*, 14190.
(7) Lever, A. B. P. *J. Chem. Soc.* **1965**, 1821.
(8) Figgis, B. M.; Nyholm, R. S. *J. Chem. Soc.* **1954**, 12.
(9) (a) Mack, J.; Stillman, M. J. in *The Porphyrin Handbook*; Kadish, K. M., Smith, K. M., Guilard, R., Eds.; Academic Press: New York, 2003; Vol. 16, pp 43−116. (b) Gouterman, M. In *The Porphyrins*; Dolphin, D., Ed.; Academic Press: New York, 1978; Vol. III, and references therein.

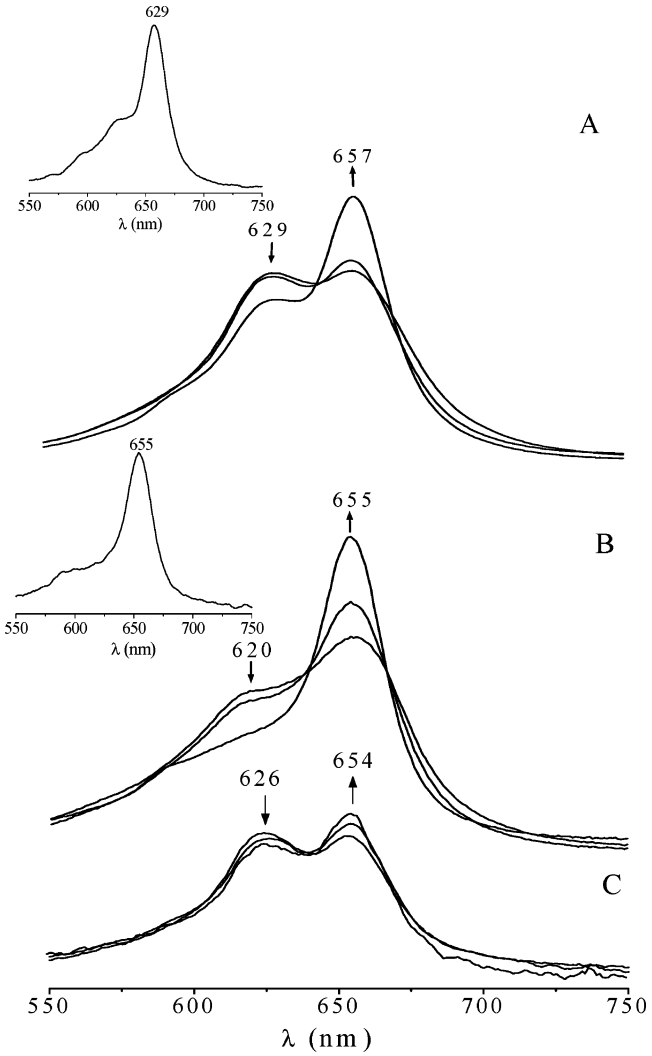


**Figure 3.** UV−visible spectra in aqueous solution at different concentrations of the hydrated species: (A) $[(2\text{-Mepy})_8\text{TPyzPzMg}(H_2O)]^{8+}$ ($c = 1.26 \times 10^{-4}-1.26 \times 10^{-6}$ M; the inset shows the spectrum at $1.26 \times 10^{-7}$ M); (B) $[(2\text{-Mepy})_8\text{TPyzPzCu}]^{8+}$ ($c = 1.01 \times 10^{-4}-1.01 \times 10^{-6}$ M; the inset shows the spectrum at $1.01 \times 10^{-7}$ M); (C) $[(2\text{-Mepy})_8\text{TPyzPzZn}]^{8+}$ ($c = 5.18 \times 10^{-6}-5.18 \times 10^{-7}$ M; higher concentrations resulted in only minimal changes with respect to the spectrum obtained at $5.18 \times 10^{-6}$ M concentration).

tion, already evidenced for the free-base cation $[(2\text{-Mepy})_8\text{TPyzPzH}_2]^{8+}$,[1] is also generally observed for the metal derivatives in water solutions.

It should be noted here that the free-base cation, which is aggregated at pH = 7, is monomeric in strongly acidic water solutions (2 N or 6 N HCl) clearly as a consequence of protonation at the pyrazine N atoms, which brings the total positive charge of the cationic macrocycle up to a formal value of 16+.[1] It is also noted that the $Cu^{II}$ and $Zn^{II}$ complexes in an acidic 2 N HCl solution (the $Mg^{II}$ complex demetalates in the same medium) show the spectral pattern expected for a monomeric form of the compound (a unique sharp Q band at 669 for $Cu^{II}$ and 675 nm for $Zn^{II}$, see Figure S1 in the Supporting Information). This indicates that while the 8+ charges located externally at the pyridine N atoms do not preclude contact between adjacent pyrazinoporphyrazine central sites, protonation of the pyrazine N atoms, accompanied by a concomitant proton interaction with the *meso* N atoms, leads to a complete disaggregation.

**(b) Pyridine, DMSO.** Table 2 lists spectral data of the four $[(2\text{-Mepy})_8\text{TPyzPzM}](I_8)$ derivatives ($M = Mg^{II}(H_2O)$, $Zn^{II}$, $Cu^{II}$, and $Co^{II}$) in pyridine and DMSO solutions along with data for the corresponding unquaternized species. The spectra of the quaternized complexes in the two solvents are very similar to each other in that they all show an unsplit narrow Q band accompanied by a B band at higher energy. These spectral features suggest $D_{4h}$ symmetry for the macrocycle, independent of the type of the $M^{II}$ center, as expected.[9] The spectra remain practically unchanged over the period of a few hours, and the intensity variations, occasionally observed, do not exceed 2−4%. These data indicate that the complexes are practically monomeric in pyridine and DMSO with only initial slight traces of detectable molecular aggregation which disappears with the time. This behavior is different from what is observed for the related $[Py_8\text{TPyzPzM}]$ complexes, which all show initially the occurrence of aggregation in pyridine[3] or DMSO and even in other low- or noncoordinating solvents.[3] It is true, however, that for the same $[Py_8\text{TPyzPzM}]$ complexes, disaggregation systematically takes place as a function of time in all of the solvents, and the monomeric forms are ultimately formed.[3]

It can be seen from Table 2 that the octacationic $[(2\text{-Mepy})_8\text{TPyzPzM}]^{8+}$ species ($M = Mg^{II}(H_2O)$, $Zn^{II}$, $Cu^{II}$, and $Co^{II}$) display a Q-band position in DMSO solutions which is shifted hypsochromically by 10−15 nm as compared to the spectra in pyridine. This systematic shift in $\lambda_Q$ may result from different axial ligation in pyridine and DMSO. An additional important observation regarding the peak position of the Q band when comparing each quaternized complex (q) and the respective unquaternized analogue (uq) in either pyridine or DMSO is that a bathochromic shift is always observed (10−20 nm) in the direction uq → q in each solvent. This shift must be ascribed to an electronic effect, probably mainly operative through the $\sigma$-bond system, and due to the quaternization of the pyridine N atoms. This is the first evidence provided by UV−visible spectra for the change which occurs in the electronic charge distribution on the entire macrocyclic framework as a result of a quaternization process at the pyridine N atoms.

**Electrochemical Measurements.** Cyclic voltammetric and spectroelectrochemical measurements were made in DMSO on the octacationic macrocycles $[(2\text{-Mepy})_8\text{TPyzPzM}]^{8+}$ ($M = Mg^{II}(H_2O)$, $Zn^{II}$, $Cu^{II}$, $Co^{II}$) in the form of the hydrated iodide salts. For appropriate comparison, the corresponding series of the neutral hydrated macrocycles $[Py_8\text{TPyzPzM}]$ ($M = Mg^{II}(H_2O)$, $Zn^{II}$, $Cu^{II}$, and $Co^{II}$, with extension to $Mn^{II}$ and $2H^{I}$) were also examined in the same solvent.

The electrochemical behavior of free-base $[Py_8\text{TPyzPzH}_2]$ and the related $[Py_8\text{TPyzPzM}]$ complexes was previously reported in pyridine solutions,[2,3] and data were also obtained in $CH_2Cl_2$ for $M = Zn^{II}$, $Cu^{II}$, and $2H^{I}$.[2,3] To compare data in the same solvent, the electrochemistry on the parallel series of positively charged $[(2\text{-Mepy})_8\text{TPyzPzM}]^{8+}$ species was also explored in pyridine. For this latter series of macro-

**Table 3.** Half-Wave Potentials[e] of the Neutral Species [$Py_8$TPyzPzM][f] and the Corresponding Octacationic Complexes [(2-Mepy)$_8$TPyzPzM]$^{8+}$ [g]

| | | | reduction | | | | | | $\Delta E_{1/2}$ | | | | |
|---|---|---|---|---|---|---|---|---|---|---|---|---|---|
| compound[a] | solvent | oxidation | first | second | | third | fourth | fifth | $\Delta_{1-2}$ | $\Delta_{2-3}$ | $\Delta_{3-4}$ | $\Delta_{4-5}$ | ref[d] |
| [$Mg^{II}$] | py | | −0.40 | −0.79 | | −1.43 | −1.70 | | 0.39 | 0.64 | 0.27 | | 3 |
| | DMSO | | −0.33 | −0.70 | | −1.39 | −1.67 | | 0.37 | 0.69 | 0.28 | | tw |
| [$Mg^{II}$]$^{8+}$ | DMSO | 0.31 | −0.19 | −0.47 | | −0.84 | −1.28 | | 0.28 | 0.37 | 0.44 | | tw |
| [$Zn^{II}$][b] | py | | −0.34 | −0.72 | | −1.38 | −1.66 | −1.83 | 0.38 | 0.66 | 0.28 | 0.17 | 3 |
| | DMSO | | −0.26 | −0.67 | | −1.38 | −1.64 | | 0.41 | 0.71 | 0.26 | | tw |
| [$Zn^{II}$]$^{8+}$ [c] | DMSO | 0.33 | −0.10 | −0.44 | | −0.81 | −1.24 | −1.59 | 0.34 | 0.37 | 0.43 | 0.35 | tw |
| [$Cu^{II}$] | py | | −0.30 | −0.68 | | −1.28 | −1.61 | | 0.38 | 0.61 | 0.33 | | 3 |
| | DMSO | | −0.22 | −0.58 | | −1.22 | −1.58 | | 0.36 | 0.64 | 0.36 | | tw |
| [$Cu^{II}$]$^{8+}$ | DMSO | 0.30 | −0.04 | −0.38 | | −0.85 | −1.22 | | 0.37 | 0.47 | 0.37 | | tw |
| [$Co^{II}$] | py | | −0.26 | −0.87 | | −1.37 | −1.83 | | 0.61 | 0.50 | 0.46 | | 3 |
| | DMSO | 0.67 | −0.06 | −0.76 | | −1.31 | −1.77 | | 0.70 | 0.55 | 0.46 | | tw |
| [$Co^{II}$]$^{8+}$ | DMSO | 0.32 | 0.05 | −0.51 | | | | | 0.57 | | | | |
| [$Mn^{II}$] | py | | −0.21 | −0.91 | | −1.35 | −1.64 | | 0.70 | 0.44 | 0.29 | | 3 |
| | DMSO | 0.36 | −0.16 | −0.89 | | −1.33 | −1.80 | | 0.73 | 0.44 | 0.47 | | tw |
| [$2H^{I}$] | $CH_2Cl_2$ | | −0.15 | −0.50 | −1.00 | −1.31 | −1.65 | | 0.35 | 0.50 | 0.31 | 0.34 | 2 |
| | py | | −0.17 | −0.48 | −0.93 | −1.24 | −1.61 | | 0.31 | 0.45 | 0.31 | 0.37 | 2 |
| | DMSO | | −0.16 | −0.40 | −0.89 | −1.21 | −1.57 | | 0.34 | 0.40 | 0.32 | 0.36 | tw |

[a] Since the complexes [$Py_8$TPyzPzM] can be obtained from either pyridine or DMSO as a solvent of reaction,[3] it is specified here that the $Zn^{II}$ and $Cu^{II}$ complexes were prepared from pyridine and the $Mg^{II}$, $Co^{II}$, and $Mn^{II}$ from DMSO. [b] A fifth reduction is seen at −1.83 V. [c] A fifth reduction is observed at −1.59 V. [d] tw = this work. [e] $E_{1/2}$, V vs SCE; 0.1 M TBAP, scan rate 100 mV/s. [f] Abbreviated in the table as [$M^{II}$] or [$2H^{I}$]. [g] Abbreviated in the table as [$M^{II}$]$^{8+}$.

cycles, however, the results were of much lower quality in terms of obtaining reversible electron transfer processes and sufficiently well-defined current voltage curves to measure meaningful half-wave potentials. On the other hand, the use of water as a medium for measurements of both series of macrocycles was not possible owing to the insolubility of the [$Py_8$TPyzPzM] species in this medium; in addition, electrochemical results for the octacationic macrocycles in aqueous solutions were not easy to interpret, for reasons probably associated with the presence of aggregation phenomena. Among the solvents examined, i.e., $H_2O$, pyridine, DMF, and DMSO, the latter appeared to be the most appropriate medium for electrochemical measurements (potential range +0.8 to −2.0 V vs SCE), and the data collected in this solvent are here presented and discussed.

It is of some interest to discuss first the electrochemical behavior of the neutral [$Py_8$TPyzPzM] macrocycles, in light of previous results obtained in pyridine,[2,3] and this is followed by a comparison of the resulting data for the octacationic [(2-Mepy)$_8$TPyzPzM]$^{8+}$ analogues.

**[$Py_8$TPyzPzM].** Electrochemical data for neutral [$Py_8$TPyzPzM] (M = $Mg^{II}(H_2O)$, $Zn^{II}$, $Cu^{II}$, $Co^{II}$, $Mn^{II}$, $2H^{I}$) in DMSO and pyridine and the parent 8+ charged species [(2-Mepy)$_8$TPyzPzM]$^{8+}$ in DMSO are summarized in Table 3. The cyclic voltammograms of each [$Py_8$TPyzPzM] complex in DMSO are depicted in Figure 4. They show in all cases four extremely well-defined reversible one-electron reductions, in line with previous findings in pyridine solutions.[3] Shown also in Figure 4 are the one-electron oxidations of the $Co^{II}$ and $Mn^{II}$ complexes, which were not not observed previously in pyridine solution[3] (see later discussion below).

Table 3 lists the $E_{1/2}$ values (V vs SCE) and the potential separations between the different stepwise reductions, listed here as $\Delta_{1-2}$, $\Delta_{2-3}$, and $\Delta_{3-4}$. It can be seen from the $E_{1/2}$ values measured for reductions in the two media (DMSO and pyridine) that there is only a slight solvent dependence on the half-wave potentials when measured vs SCE or vs

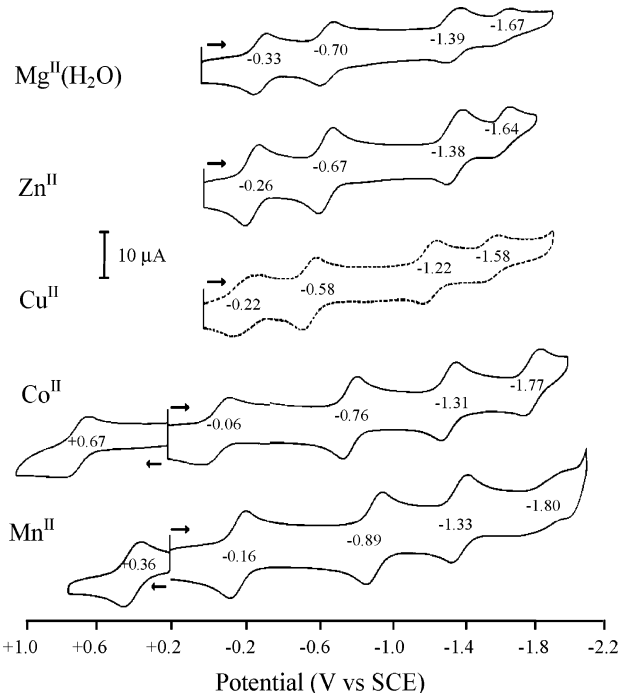


**Figure 4.** Cyclic voltammograms, with added $E_{1/2}$ values (V vs SCE), of [$Py_8$TPyzPzM] complexes (ca. $10^{-4}$ M) in DMSO, 0.1 M TBAP; scan rate = 200 mV/s (— first scan; - - - - second scan).

$Fc^+$/Fc. Nevertheless, the $E_{1/2}$ values in DMSO are systematically a little less negative than those for the corresponding reductions in pyridine, with $\Delta E_{1/2} \leq 0.11$ V when measured vs SCE for all reactions, except the first reduction of $Co^{II}$ (where $\Delta E_{1/2} = 0.20$ V) and the fourth reduction of $Mn^{II}$ (where $\Delta E_{1/2}$ differs in an opposite direction, i.e., $\Delta E_{1/2} = -0.16$ V). The $E_{1/2}$ of the $Fc^+$/Fc couple was measured under our experimental conditions as 0.50 V vs SCE in DMSO and 0.55 V in pyridine, and this leads to the conclusion that all reductions steps are generally favored in DMSO. For each [$Py_8$TPyzPzM] species, similar values of $\Delta_{1-2}$, $\Delta_{2-3}$, and $\Delta_{3-4}$ are found in pyridine and DMSO, the values in most

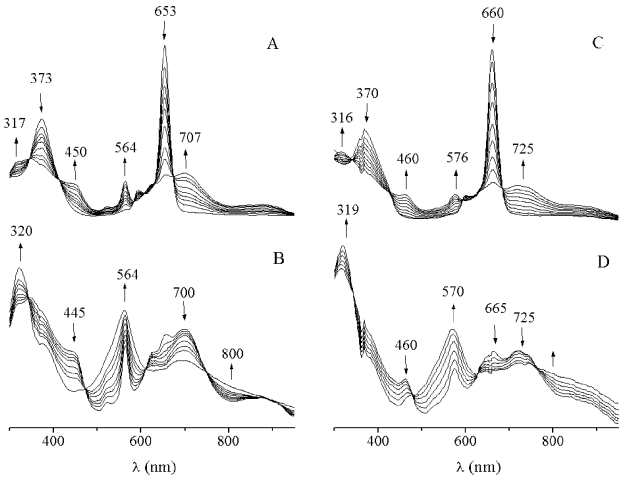


**Figure 5.** UV−visible spectral changes in DMSO containing 0.2 M TBAP during controlled potential electrolysis of $[Py_8TPyzPzMg(H_2O)]$ at (A) −0.56 V (first reduction) and (B) −1.0 V (second reduction) and of $[(2\text{-}Mepy)_8TPyzPzMg(H_2O)]^{8+}$ at (C) −0.35 V (first reduction) and (D) −0.70 V (second reduction).

cases differing by no more than 0.05 V. This indicates that identical stepwise reduction processes must occur in the two solvents.

**M = Mg$^{II}$, Zn$^{II}$, Cu$^{II}$.** The $E_{1/2}$ values in DMSO, as in pyridine,[3] become progressively more positive in the sequence $Mg^{II} < Zn^{II} < Cu^{II}$ for each reduction step with practically no exceptions (Table 3). If only the first reduction is considered, inclusion of the $Co^{II}$ and $Mn^{II}$ species leads to the sequence $Mg^{II} < Zn^{II} < Cu^{II} < Mn^{II} < Co^{II}$ in DMSO. Again the latter two complexes are more easily reduced than in pyridine although in pyridine they are found in a reverse order: $Co^{II} < Mn^{II}$. As to the second, third, and fourth reductions of the $Mn^{II}$ and $Co^{II}$ species, they show $E_{1/2}$ values definitely more negative than those of the $Cu^{II}$ derivative, i.e., the $Mn^{II}$ and $Co^{II}$ species are less easily reduced after the first reduction.

The sequence of reduction processes $[Py_8TPyzPzM]^{0/1-/2-/3-/4-}$ found in DMSO for the $Mg^{II}$, $Zn^{II}$, and $Cu^{II}$ complexes, owing to the electroinactive metal centers, is obviously assumed to be ligand-centered at all steps of the reduction. The well-outlined profile of the one-electron processes and the observed good reversibility (Figure 4) signify that the uptake of electrons is facilitated by the electron deficiency of the entire macrocycle, with stabilization, through a $\sigma/\pi$-electron mechanism of delocalization, of the negatively charged species formed.

The spectroelectrochemical behavior of the $Mg^{II}$, $Zn^{II}$, and $Cu^{II}$ species in DMSO shows similar trends during the multistep reductions. The thin-layer spectral changes obtained during the first and second reductions are depicted for the $Mg^{II}$ derivative in Figure 5 (parts A and B, respectively).

The spectral changes observed for the two stepwise reductions are similar to those observed previously in pyridine,[3] namely the disappearance of the Q band upon the first one-electron reduction (Figure 5A) and the appearance of an absorption at ca. 564 nm in the second reduction step (Figure 5B), with concomitant changes above 700 nm and in the Soret region. Both sets of spectral changes are reversible and give back the original spectra upon stepwise reoxidation (see Figure S2(A,B), Supporting Information).

Similar to what was seen in pyridine,[3] no oxidations are observed in DMSO for the $[Py_8TPyzPzM]$ complexes with $Mg^{II}$, $Zn^{II}$, or $Cu^{II}$ metal ions, as expected since these metal centers are electroinactive. In addition, ring-centered oxidations should be observed at highly positive potentials, well beyond the solvent potential limit, owing to the electron deficiency of the ligand framework and consequent low tendency of the three above complexes to release electrons with formation of positively charged radicals. This is different from what occurs for the "diazepinoporphyrazine" complexes, $[Ph_8DzPzM]$,[6] which are electrooxidized to give $\pi$-cation radicals in $CH_2Cl_2$ or pyridine at potentials > 0.5 V vs SCE with M = $Zn^{II}$ ($CH_2Cl_2$, 0.65 and 1.03 V; pyridine, 0.64 and 0.96 V), $Cu^{II}$ (pyridine, 0.76 V), $Co^{II}$ ($CH_2Cl_2$, 1.11 V; pyridine, 1.10 V), and $Mn^{II}$ ($CH_2Cl_2$, 1.35 V), thus suggesting that these macrocycles are less electron-deficient than the currently discussed "pyrazinoporphyrazine" species.

**M = Co$^{II}$, Mn$^{II}$, 2H$^{I}$.** Although the same stepwise reduction sequence is also proposed to occur for the $Mn^{II}$ derivative as for the $Mg^{II}$, $Zn^{II}$, and $Cu^{II}$ species in DMSO, the mechanism for reduction of the $Co^{II}$ complex follows a quite different pathway, as shown in eqs 1 and 2. Here the central $Co^{II}$ ion is reduced to its $Co^{I}$ form in the first step, and the $Co^{II}$ dianion is formed after addition of a second electron.

$$[Py_8TPyzPzCo^{II}] + e^- \rightleftharpoons [Py_8TPyzPzCo^{I}]^- \qquad (1)$$

$$[Py_8TPyzPzCo^{I}]^- + e^- \rightleftharpoons [Py_8TPyzPzCo^{II}]^{2-} \qquad (2)$$

This proposed reduction mechanism in DMSO parallels a mechanism previously postulated to occur for the same species in pyridine[3] and is in line with similar findings for the phthalocyanine analogue [PcCo] in DMSO,[10] pyridine,[11] or THF.[12] Thin-layer UV−visible spectral changes associated with the first and second reductions and reverse reoxidation processes in DMSO are similar to what was reported to occur in pyridine[3] (hence, not shown here again), leaving little doubt that the same mechanistic sequence of reduction steps (eqs 1 and 2) also takes place in DMSO.

One striking difference in the electrochemical behavior of the $Co^{II}$ and $Mn^{II}$ complexes in DMSO as compared to pyridine is that one-electron reversible oxidations are observed in DMSO at $E_{1/2}$ values of +0.67 and +0.36 V vs SCE, respectively (see Figure 4 and Table 3), whereas no redox processes could be detected in this anodic region in pyridine.[3] It is postulated that the higher donor properties of the pyridine molecule with respect to DMSO makes higher the redox potential of the $M^{III}/M^{II}$ couple in pyridine, so that in this medium the $M^{II}$ oxidation state is favored for both complexes. The higher $E_{1/2}$ value for the $Co^{II}$ complex with respect to the $Mn^{II}$ species in DMSO is consistent with results

(10) Stillman, M. J.; Thomson, A. J. *J. Chem. Soc., Faraday Trans. 2* **1974**, *70*, 790.
(11) Day, P.; Hill, H. A. O.; Price, M. G. *J. Chem. Soc. A* **1968**, 90.
(12) Clack, D. W.; Hush, N. S.; Woolsey, I. S. *Inorg. Chim. Acta* **1976**, *19*, 129.

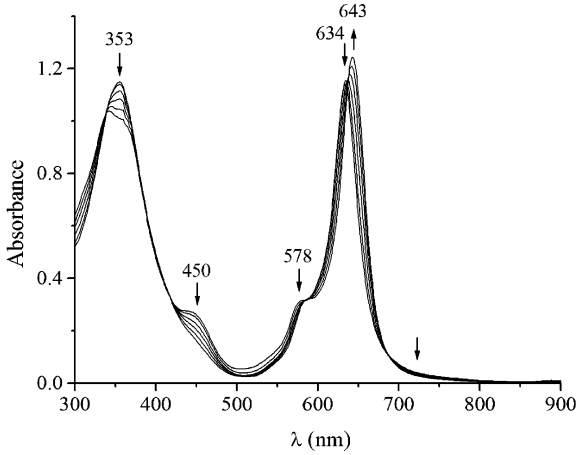


**Figure 6.** UV−visible spectral changes in DMSO containing 0.2 M TBAP during controlled potential electrolysis of [$Py_8$TPyzPzCo] at +0.80 V (first oxidation).

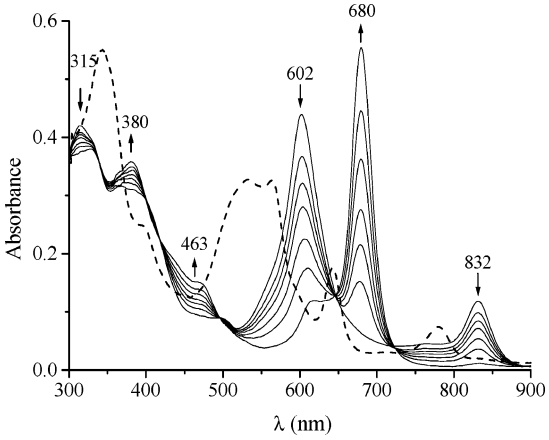


**Figure 7.** UV−visible spectral changes in DMSO containing 0.2 M TBAP during controlled potentials electrolysis of [$Py_8$TPyzPzMn] at +0.60 V (first oxidation). The figure shows also the spectrum of the $Mn^{II}$ complex in pyridine (dashed line).

obtained for the same metal-centered oxidations in the previously studied "diazepinoporphyrazine" $Co^{II}$ ($CH_2Cl_2$: 0.66 V; pyridine, 0.64 V) and $Mn^{II}$ ($CH_2Cl_2$, −0.05 V; pyridine, −0.20 V) complexes.[6]

The changes in UV−visible spectra upon oxidation of the $Co^{II}$ and $Mn^{II}$ species deserve some comments. The spectrum of the neutral [$Py_8$TPyzPzCo$^{II}$] complex (d,[7] low spin) in DMSO shows only subtle differences from the spectrum in pyridine[3] (Table 2). The observed changes upon the one-electron oxidation (Figure 6) to form the 1+ charged species [$Py_8$TPyzPzCo$^{III}$]$^+$ consist of a small bathochromic shift (634 → 643 nm) and a slight change in intensity of the Q band, accompanied by only additional minor variations below 500 nm. This indicates that the change in the oxidation state of the metal only weakly affects the macrocyclic $\pi$ system. Several isosbestic points are seen, indicating the lack of any spectrally detectable intermediates. The reverse process regenerates the initial UV−visible spectrum. It should be noticed here that minor spectral changes are also observed for the $Co^{II}/Co^{III}$ redox process of related porphyrin[13] and phthalocyanine[14] macrocycles.

The UV−visible spectra of the $Mn^{II}$ species in DMSO and pyridine and the spectral variations which occur in DMSO upon controlled potential oxidation at +0.60 V are shown in Figure 7. First, it must be noted that the unoxidized complex shows "normal" spectral features in DMSO as expected for a complex of $D_{4h}$ symmetry, i.e., there is a single Q band (maximum at 602 nm) and absorptions of comparable or lower intensity in the Soret region plus additional lower intensity peaks at 832 and ca. 500 nm. The spectrum in pyridine is quite different. It shows a broad intense envelope in the spectral window of 500−600 nm with maxima at 532 and 564 nm and a weak Q band at 644 nm. There are also low intensity absorptions at ca. 400 and 783 nm and a high intensity absorption in the Soret region (346 nm). These spectral features (which are also present in 4-methylpyridine) were previously discussed[3] and are associated with the presence of a six-coordinate low-spin complex which forms in solution as a result of axial ligation by pyridine. The broad envelope in the 500−600 nm region was assigned as a Mn → L (ligand) or L → Mn charge transfer, in analogy with similar assignments for the $Mn^{II}$ phthalocyanine complex, [PcMn], in the form of its bis-*N*-methylimidazole adduct, [PcMn(N-MeIm)$_2$].[15] It seems plausible that [$Py_8$TPyzPzMn], which is high-spin in the solid state ($\mu_{eff} = 5.46\ \mu_B$ at room temperature[3]) retains its high-spin state in DMSO, owing to the relatively low donor properties of this latter solvent as compared to pyridine. If this is the case, then, evidently the charge-transfer band is not allowed for $Mn^{II}$ in its high-spin state, and the spectrum shows its "normal" pattern.

The UV−visible spectral changes observed in DMSO upon the first one-electron oxidation of [$Py_8$TPyzPzMn$^{II}$] to form [$Py_8$TPyzPzMn$^{III}$]$^+$ (Figure 7) consist of a considerable bathochromic shift of the Q band from 602 to 680 nm and a B band which is shifted from 315 to 380 nm. A disappearance of the absorption at 832 nm is also observed, and further changes occur in the spectral region 450−500 nm. These spectral variations are reversible as seen by reduction of the 1+ charged species to regenerate the neutral complex. The bathochromic shift of the Q and B bands upon oxidation of $Mn^{II}$ to $Mn^{III}$ is clearly indicative of a remarkable decrease of the HOMO−LUMO energy level separation and probably is related to the fact that the $Mn^{II}$ complex ($d^5$) is in a high-spin state with the unpaired electrons spread over all the d orbital levels of the metal center. Undoubtedly therefore, upon the metal-centered $Mn^{II} \rightarrow Mn^{III}$ oxidation, the one-electron release leads to such a rearrangement of the electronic structure of the metal center so that significant effects are produced in the $\sigma$- and especially the $\pi$-electron distribution within the ligated macrocycle.

(13) D'Souza, F.; Villard, A.; Van Caemebecke, E.; Franzen, M.; Boschi, T.; Tagliatesta, P. and Kadish, K. M. *Inorg. Chem.* **1993**, *32*, 4042.
(14) (a) L'Her, M.; Pondaven, A. In *The Porphyrin Handbook;* Kadish, K. M., Smith, K. M., Guilard, R., Eds.; Academic Press: Amsterdam, 2003; Vol. 16, Chapter 104, p 117. (b) Lever, A. B. P.; Milaeva, E. R.; Speier, G. *Phthalocyanines − Properties and Applications*; Leznoff, C. C., Lever, A. B. P., Eds.; VCH Publishers: New York, 1993; Vol. 3, pp 1−69.
(15) Wilshire, J. P.; Lever, A. B. P. Unpublished data. See Stillman, M. J. In *Phthalocyanines − Properties and Applications*; Leznoff, C. C., Lever, A. B. P., Eds.; VCH Publishers Inc.: New York, 1989; Vol. 1, pp 204−205.

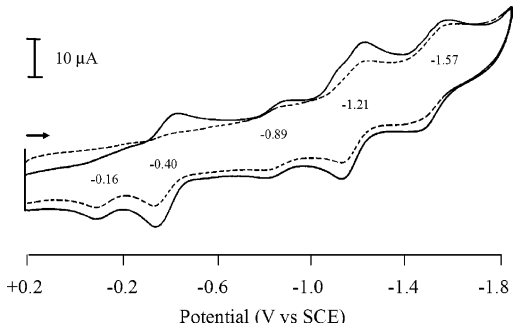


**Figure 8.** Thin layer cyclic voltammogram, with added $E_{1/2}$ values, of $[Py_8TPyzPzH_2]$ (ca. $10^{-4}$ M) in DMSO, 0.2 M TBAP; scan rate = 20 mV/s (- - - - first scan; — second scan).

The cyclic voltammetric behavior of free-base $[Py_8TPyzPzH_2]$ is characterized by five reductions in pyridine or $CH_2Cl_2$ and was previously discussed in detail.[2] It was established that four of the five one-electron reductions which occur in both solvents, i.e., the first, second, fourth, and fifth reduction processes (−0.15/−0.17, −0.50/−0.48, −1.31/−1.24−1.65/−1.61 V vs SCE, Table 3) are due to electron uptake by the neutral species, whereas the third electron-transfer process (−1.00/−0.93 V) is due to a reduction of the deprotonated dianion $[Py_8TPyzPz]^{2-}$, which is generated via the equilibrium given by eq 3.

$$[Py_8TPyzPzH_2] \rightleftharpoons [Py_8TPyzPz]^{2-} + 2H^+ \qquad (3)$$

The ensemble of the electron transfer processes in DMSO, as evidenced by the cyclic voltammograms shown in Figure 8, substantially conforms to what is seen in pyridine or $CH_2Cl_2$, and it seems plausible that, as previously discussed in detail,[3] the same conclusions can be drawn from the data in DMSO, namely the first, second, fourth, and fifth reductions are assigned to the neutral species and the third one to the corresponding deprotonated species. The sequence of the $E_{1/2}$ values, which are systematically a little lower than those in pyridine (Table 3), may be taken as indicative that the reductions are more facile in DMSO than in pyridine or $CH_2Cl_2$, in line with findings for the metal derivatives $[Py_8TPyzPzM]$, as outlined above.

**$[(2\text{-Mepy})_8TPyzPzM]^{8+}$.** The electrochemical behavior of the octacationic $[(2\text{-Mepy})_8TPyzPzM]^{8+}$ macrocycles (as hydrated iodide salts) was examined in DMSO under experimental conditions similar to those for measurements of the unquaternized $[Py_8TPyzPzM]$, thus enabling a good comparison between the two sets of data. It was expected that the cyclic voltammetric patterns of the 8+ charged macrocycles might show profiles resembling those observed for the neutral species, although complicated by the interfering presence of reductions associated with the 1+ charged pyridine N atoms and oxidations of the $I^-$ counterions.

It is known that redox processes of the $2I^-/I_2$ couple should occur at potentials between 0.0 and 0.7 V vs SCE, and this was confirmed under our experimental conditions by measuring the oxidation of KI in DMSO containing 0.1 M TBAP (see discussion below). As to the *N*-methylpyridiniumyl rings, literature data indicate that unresolved multielectron reductions are observed at potentials close to −1.20 V vs SCE for tetramethylated tetrapyridinoporphyrazine complexes in which the $N^+$ atoms belong to pyridine rings directly annulated to the central porphyrazine core.[16] A number of studies[17] have been conducted on different series of metal complexes of the tetracationic *meso*-tetrakis(*N*-methylpyridiniumyl)porphyrin, in which four *N*-methylated pyridine rings are appended in the *meso* positions of the porphyrin macrocycle and, hence, share, in this respect, some similarity to the cationic units in the present complexes. It has been seen that multistep reductions of the *N*-methylpyridiniumyl rings generally occur in the range of potentials from −0.80 to −1.30 V vs SCE. To our knowledge, there is only one report in the literature dealing with an octacationic porphyrazine macrocycle with eight externally appended *N*-methylpyridiniumyl rings, but no electrochemical data were reported.[18]

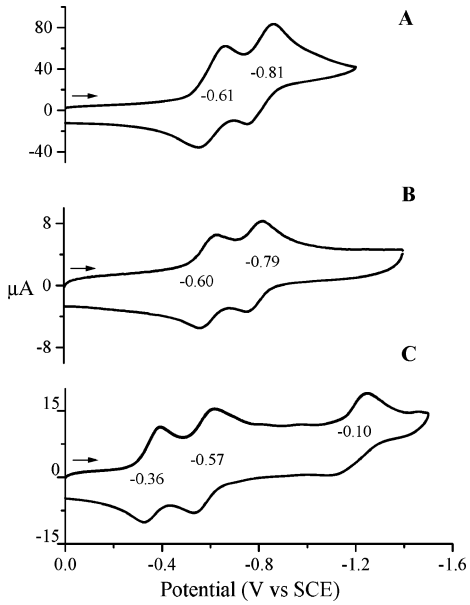


**Figure 9.** Cyclic voltammograms, with added $E_{1/2}$ values in DMSO ($c \sim 10^{-3}$ M; 0.1 M TBAP) of (A) $[(CN)_2Py(2\text{-Mepy})Pyz](I)$, (B) $[(CN)_2Py(2\text{-Mepy})Pyz](OTs)$, and (C) $[(CN)_2(2\text{-Mepy})_2Pyz](OTs)_2 \cdot 4H_2O$ (scan rate 100 mV/s).

To obtain additional pertinent information, the available[1] mono- and diquaternized species, $[(CN)_2Py(2\text{-Mepy})Pyz](I)$, $[(CN)_2Py(2\text{-Mepy})Pyz](CH_3C_6H_4SO_3)$, and $[(CN)_2(2\text{-Mepy})_2Pyz](CH_3C_6H_4SO_3)_2$, were examined by cyclic voltammetry in DMSO, 0.1 M TBAP. The voltammograms are shown in Figure 9. The monocation $[(CN)_2Py(2\text{-Mepy})Pyz]^+$, either as iodide or *p*-toluenesulfonate salt, shows two reversible reductions at ca. −0.60 and ca. −0.80 V vs SCE, whereas the dication $[(CN)_2Py(2\text{-Mepy})Pyz]^{2+}$ exhibits three reversible reductions, two at considerably more positive potentials than those for the monocation, i.e. −0.36 and −0.57 V vs SCE, and a third reduction which occurs at a more negative

(16) (a) Smith, T. D.; Livorness, J.; Taylor, H.; Pilbrow, J. R.; Sinclair, G. R. *J. Chem. Soc., Dalton Trans.* **1983**, 1391. (b) Sekota, M.; Nyokong, T. *J. Porphyrins Phthalocyanines* **1999**, *3*, 477.

(17) Van Caemelbecke, E.; Derbin, A.; Hambright, P.; Garcia, R.; Doukkali, A.; Saoiabi, A.; Ohkubo, K.; Fukuzumi, S.; Kadish, K. M. *Inorg. Chem.* **2005**, *44*, 3739, and references therein.

(18) Anderson, M. E.; Barrett, A. G. M.; Hoffman, B. M. *Inorg. Chem.* **1999**, *38*, 6143.

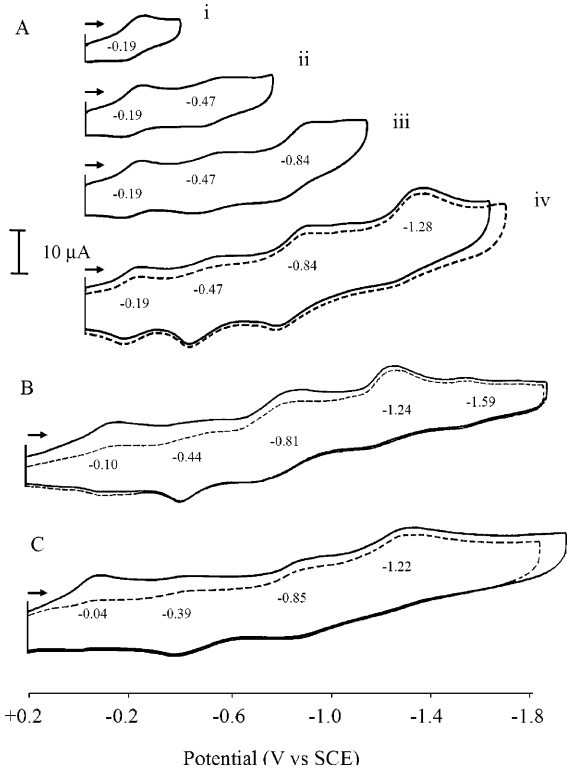


**Figure 10.** Cyclic voltammograms, with added $E_{1/2}$ values of (A) [(2-Mepy)$_8$TPyzPzMg(H$_2$O)]$^{8+}$, (B) [(2-Mepy)$_8$TPyzPzZn]$^{8+}$, and (C) [(2-Mepy)$_8$TPyzPzCu]$^{8+}$ in DMSO ($c \sim 10^{-4}$ M); 0.1 M TBAP, scan rate 200 mV/s (in A-iv, B, and C, the dashed line refers to the first and the solid line to the second scan).

potential (−1.10 V vs SCE). Neither the monocation nor the dication (as *p*-toluenesulfonate salts) show oxidation processes in the anodic region (+0.8 to 0.0 V vs SCE). Moreover, it was shown by our experiments that the *p*-toluenesulfonate anion (as a sodium salt) is electrochemically inactive, and thus no interference by this anion is expected within the potential region explored (+0.8 to −2.0 V vs SCE). The observed differences between the monocation and the dication in terms of number of reductions and $E_{1/2}$ values suggest that the two $NCH_3^+$ moieties of the dication are not independent of each other; rather, they seem to be electronically interrelated through the connecting pyrazine ring. A detailed interpretation of the reduction behavior of these species is out of the scope of the present work. Nevertheless, the wide range of observed $E_{1/2}$ values extended from −0.36 to −1.10 V vs SCE suggests that even a wider range of negative potentials in DMSO should be expected by the reduction of the eight $NCH_3^+$ groups present in the currently investigated octactationic macrocycles. As to the iodide of the monocation, the pattern attributable to the oxidation of the $I^-$ ion is observed in DMSO, in keeping with expectation, with $E_{1/2}$ values of +0.30 and +0.63 V vs SCE (not shown). This set of data will be of some utility for the following discussion on the electrochemistry of the present series of octacationic species.

**M = Mg$^{II}$ and Zn$^{II}$.** Figure 10A(i−iv) shows cyclic voltammograms of the octacation [(2-Mepy)$_8$TPyzPzMg(H$_2$O)]$^{8+}$ in the reduction region from 0.0 to −1.7 V. Four fairly well-defined, although not cleanly resolved, reductions

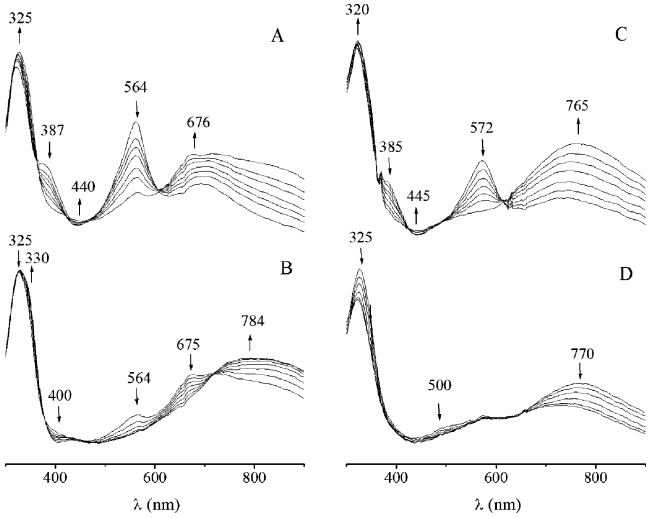


**Figure 11.** UV−visible spectral changes in DMSO containing 0.2 M TBAP during controlled potentials electrolysis of [Py$_8$TPyzPzMg(H$_2$O)] at (A) −1.60 V (third reduction) and (B) −1.90 V (fourth reduction) and of [(2-Mepy)$_8$TPyzPzMg(H$_2$O)]$^{8+}$ at (C) −1.00 V (third reduction) and (D) −1.50 V (fourth reduction).

are found at $E_{1/2}$ values of −0.19, −0.47, −0.84, and −1.28 V. The overall pattern within the cathodic potential range explored is reminiscent of that is observed for the corresponding [Py$_8$TPyzPzMg(H$_2$O)] derivative (Figure 4). Spectroelectrochemical measurements unequivocally prove that the reductions in Figure 10 involve the stepwise one-electron uptake of electrons by the macrocycle, forming, sequencially, cations [(2-Mepy)$_8$TPyzPzMg(H$_2$O)]$^{7+/6+/5+/4+}$. The related thin-layer spectral changes for the first two reductions at −0.19 and −0.47 V are depicted in Figure 5C,D and are associated with formation of [(2-Mepy)$_8$TPyzPzMg(H$_2$O)]$^{7+}$ and [(2-Mepy)$_8$TPyzPzMg(H$_2$O)]$^{6+}$. Several isosbestic points are seen, and the processes are reversible upon reoxidation (see Figure 5S2(C,D), Supporting Information). This closely parallels what is observed for reduction of the related neutral species [Py$_8$TPyzPzMg(H$_2$O)] in the same solvent (Figure 5A,B). Moreover, no interference is apparently seen in the observed spectral behavior from the concomitant redox processes of the methylated pyridine N atoms.

As is shown in Figure 5, all absorptions which appear in the spectra of electroreduced [(2-Mepy)$_8$TPyzPzMg(H$_2$O)]$^{7+,6+}$ (Figure 5C,D) are bathochromically shifted by 10−20 nm with respect to the spectra of the corresponding electroreduced unmethylated species, i.e., [Py$_8$TPyzPzMg(H$_2$O)]$^{1-,2-}$ (Figure 5A,B). This is in line with the similar bathochromic effects found for the pairs of neutral and 8+ charged species.

Figure 11 shows thin layer spectral changes which were obtained in DMSO for the third and fourth reductions of the unquaternized and quaternized Mg$^{II}$ complexes. Both sets of reductions show substantial reversibility (see Figure S3(A−D) for the stepwise reoxidations, Supporting Information). The third reductions lead to formation of the charged species [Py$_8$TPyzPzMg(H$_2$O)]$^{3-}$ and [(2-Mepy)$_8$TPyzPzMg(H$_2$O)]$^{5+}$ and are associated with quite similar spectral changes (Figure 11 (parts A and C, respectively)), except for a weak band at 676 nm in Figure 11A which is not seen in Figure 11C and which disappears during the fourth

**Table 4.** Data on the Redox Behavior of the $[M^{II}]^{8+}$ Complexes in the Reduction Region

| redox scans | residual amount of complex (%) after scans (time, min) | | | |
|---|---|---|---|---|
| | $[Mg^{II}]^{8+}$ | $[Zn^{II}]^{8+}$ | $[Cu^{II}]^{8+}$ | $[Co^{II}]^{8+}$ |
| first | 91 (49) | 82 (23) | 51 (18) | 91 (21) |
| first, second | 93 (31) | 73 (23) | 45 (31) | 96 (32) |
| first, second, third | 90 (38) | 71 (42) | 44 (35) | |
| first, second, third, fourth | 87 (54) | 70 (47) | 47 (47) | |

reduction (Figure 11B). A more appreciable difference is seen by comparison of the fourth reductions, since the broad band with maximum intensity near 800 nm, which increases in Figure 11B, reverses its intensity in Figure 11D. It is plausible that these differences might be related to some reduction of the $NCH_3^+$ pyridine moiety, being in a range of negative potentials compatible with such reductions. However, it is again pointed out that the clear appearance of electrochemical effects due to involvement of the peripheral positively charged N atoms is not seen.

Table 4 lists the residual amount (%) of 8+ charged complexes after the first thin-layer one-electron reduction and reoxidation and related total time required (min), and similar data for first → second, first → second → third, and first → second → third → fourth sequenced reductions and associated backword processes. Total reduction and reoxidation of $[Mg^{II}]^{8+}$ shows only a 14% loss of the complex (calculated by using as reference the absorbance of the Q-band peak) against a value of 7% for the neutral complex.

The cyclic voltammogram of the cationic $Zn^{II}$ complex $[(2\text{-Mepy})_8\text{TPyzPzZn}]^{8+}$ in DMSO (Figure 10B) has a general profile of the type seen for the $Mg^{II}$ analogue; there are four reductions at −0.10, −0.44, −0.81, and −1.24 V, plus one additional reduction at −1.59 V (Table 3). The total redox process, i.e., the first four reductions and back oxidations, are accompanied by a marked loss of material (30%, Table 4) which is markedly higher than for the $Mg^{II}$ octacation. Thin-layer spectral changes for the $Zn^{II}$ complex closely reproduce those seen for the $Mg^{II}$ analogue and therefore are not reported.

**M = $Cu^{II}$.** Monitoring of the thin-layer UV−visible spectral changes accompanying the first one-electron reduction of $[(2\text{-Mepy})_8\text{TPyzPzCu}]^{8+}$ followed by the reverse process indicates a significant loss of material (ca. 50%, Table 4), and, accordingly, the cyclic voltammograms show that $i_{pc} > i_{pa}$ (Figure 10C). Despite this occurrence, four stepwise one-electron reductions can again be seen, and, although they are ill-defined, they show $E_{1/2}$ values close to those of the $Mg^{II}$ and $Zn^{II}$ analogues (Table 3). The thin-layer spectral changes for the $Cu^{II}$ complex also follow trends similar to those of the $Mg^{II}$ and $Zn^{II}$ octacations. In summary, the above three species undergo a similar sequence of redox processes in the overall reduction region with a resulting relative stability of the products following the order $[Mg^{II}]^{8+} > [Zn^{II}]^{8+} > [Cu^{II}]^{8+}$. Based in large part on the spectroelectrochemical data and the known strong involvement of the macrocyclic ligand in the examined processes, the stepwise reductions can in all cases be assigned as macrocycle-centered, as is expected, owing to the well-established electrochemical inactivity of the metal centers and similar findings for the corresponding unquaternized species.

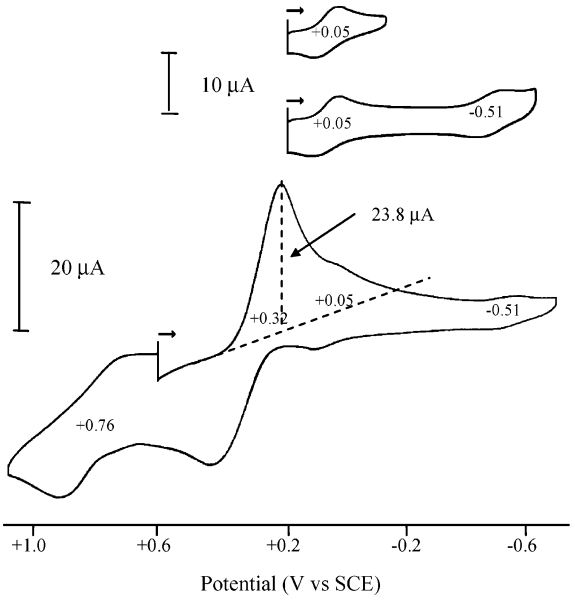


**Figure 12.** Cyclic voltammograms, with added $E_{1/2}$ values, of $[(2\text{-Mepy})_8\text{TPyzPzCo}]^{8+}$ (~$10^{-4}$ M) in DMSO, 0.1 M TBAP; scan rate = 200 mV/s.

**M = $Co^{II}$.** As shown in Figure 12, the cyclic voltammograms of the $Co^{II}$ cation $[(2\text{-Mepy})_8\text{TPyzPzCo}]^{8+}$ in DMSO exhibit two reversible well-resolved one-electron reductions at +0.05 and −0.51 V. At more negative potentials, however, several ill-defined processes occur which are difficult to analyze. The first and second reductions and the reverse processes were monitored as to their thin-layer spectral changes, which closely parallel what is seen for the unquaternized $Co^{II}$ derivative in DMSO (see discussion above) and has already been discussed for the latter species in pyridine (see Figure 9A,B in ref 3).

These changes are consistent with the processes reported in the eqs 1 and 2 and imply a conversion of $Co^{II}$ to $Co^{I}$ in the first reduction, with the second electron addition which reverses the metal-centered reduction leading to a product where the two added electrons are localized on the macrocyclic ligand.

**Electrochemical Information on *N*-Methylpyridiniumyl Rings and $I^-$ Ions.** Surprisingly, there appears to be no unequivocal processes attributable to the reduction of the *N*-methylpyridiniumyl moieties in the cathodic region. It might be that they are loosely dispersed along a wide range of potentials, and hence they are not easily observed. The general aspect of the cathodic response of the $Mg^{II}$ octacation (Figure 10A), which has a general profile undoubtedly less well-defined than that of the neutral species (Figure 4, top), is probably indicative of such a fragmented uptake and release of electrons by the *N*-methylpyridiniumyl moieties. The other possibility is that in the present octacationic macrocycles the reductions of the $NCH_3^+$ moieties are shifted to very negative potentials out of the solvent potential window.

As to $I^-$ ions, blank experiments were carried out in DMSO using potassium iodide (see above). For the present

$[(2\text{-Mepy})_8\text{TPyzPzM}]^{8+}$ species, redox processes in DMSO involving the $2I^-/I_2$ couple are found at potentials from 0.0 to +0.8 V vs SCE. A quantitative estimate of the number of exchanged electrons for $I^-$ ion was made for the 8+ charged $Co^{II}$ complex. Figure 12 shows the redox behavior of $[(2\text{-Mepy})_8\text{TPyzPzCo}](I_8)$ in the range 0.0 to +1.0 V vs SCE when the potential is scanned in a negative direction starting from +0.6 V and also from 0.00 V in the same negative direction. On the basis of the relationship $i \propto n^{3/2}$ where $i$ is the peak current ($\mu$A) and $n$ is the number of electrons, then the calculated value of $i$ is 22.6 $\mu$A for $n = 8$. The experimental value obtained (23.8 $\mu$A, Figure 12) compares well with a calculated value of 22.6 $\mu$A, which confirms the presence of eight $I^-$ ions in the cobalt complex.

**Further Comments and Conclusions.** As can be seen from Table 3, the first reduction of the cationic $Mg^{II}$ complex $[(2\text{-Mepy})_8\text{TPyzPzMg}^{II}(H_2O)]^{8+}$ occurs at −0.19 V vs SCE, and the corresponding reductions of the $Zn^{II}$ and $Cu^{II}$ analogues are at slightly less negative potentials (−0.10 and −0.04 V vs SCE, respectively). Thus, more facile first reductions occur in the sequence $Mg^{II} < Zn^{II} < Cu^{II}$. This type of sequence is maintained also for second, third, and fourth reductions, with only one exception ($Cu^{II}$, third reduction). The sequence of reductions is given in eqs 4−7 and parallels that found for the unquaternized species. It can also be extended to include the $Co^{II}$ species as far as the first reduction (Table 3).

$$[(2\text{-Mepy})_8\text{TPyzPzM}]^{8+} + e^- \rightleftharpoons [(2\text{-Mepy})_8\text{TPyzPzM}]^{7+} \quad (4)$$

$$[(2\text{-Mepy})_8\text{TPyzPzM}]^{7+} + e^- \rightleftharpoons [(2\text{-Mepy})_8\text{TPyzPzM}]^{6+} \quad (5)$$

$$[(2\text{-Mepy})_8\text{TPyzPzM}]^{6+} + e^- \rightleftharpoons [(2\text{-Mepy})_8\text{TPyzPzM}]^{5+} \quad (6)$$

$$[(2\text{-Mepy})_8\text{TPyzPzM}]^{5+} + e^- \rightleftharpoons [(2\text{-Mepy})_8\text{TPyzPzM}]^{4+} \quad (7)$$

Comparison of the experimental $E_{1/2}$ values for the stepwise reductions of the $Mg^{II}$, $Zn^{II}$, and $Cu^{II}$ unquaternized species in DMSO and the parallel series of octacationic macrocycles in the same solvent shows that the half-wave potentials for the latter series of compounds are systematically less negative than those of the neutral species, i.e., the 8+ charged species are definitely more easily reduced at all steps of reduction. Moreover, the $\Delta E_{1/2}$ values between the third and fourth reductions are larger than those for the first and second reductions. For the $Mg^{II}$ complex and its 8+ charged corresponding species, for instance, the difference in the $E_{1/2}$ values is 0.14 V for the first reduction and 0.23 V for the second reduction but becomes larger, i.e., 0.55 and 0.39 V, for the third and fourth reductions, respectively. A similar trend in $E_{1/2}$ values is observed for the $Zn^{II}$ (0.16, 0.23, 0.57, 0.40 V) and $Cu^{II}$ species (0.21, 0.20, 0.37, 0.36 V). The same level of comparison cannot be extended to the $Co^{II}$ and $Mn^{II}$ complexes for lack of data. It is true, however, that also for the $Co^{II}$ species, the octacationic macrocycle is more easily reduced in the first and second one-electron addition processes. These results clearly indicate that the quaternization process at the external pyridine N atoms significantly modifies the general $\sigma/\pi$ electronic distribution over the entire macrocycle, appended pyridine rings included, in such a way that the electron-deficient properties of the quaternized species are enhanced with significant effects on the general electrochemical properties. To our knowledge, this is the first time that such effects have been observed in macrocyclic systems, either porphyrinic or porphyrazinic, with induced electronic effects determined by moieties located at such a long distance from the central porphyrazine core.

The new quaternized porphyrazine materials described in the present and companion[1] papers as well as the corresponding unquaternized species[2,3] may be promising materials for investigating their possible interactions with nucleic acids or for their use as photosensitizers in photodynamic therapy.

**Acknowledgment.** Financial support by the University of Rome La Sapienza and the MIUR (Cofin 2003038084) and the Robert A. Welch Foundation (K.M.K., Grant E-680) is gratefully acknowledged. M.P.D. thanks the Department of Chemistry, Houston University, for kind hospitality. Thanks are expressed to M. Occhiuzzi, F. Scannerini, M. Manni, and M. Corsini for experimental help and to Prof. P. A. Stuzhin and Dr. P. Galli for suggestions and useful discussions.

**Supporting Information Available:** UV−visible spectra of $[(2\text{-Mepy})_8\text{TPyzPzM}](I_8)$ (M = $Zn^{II}$ and $Cu^{II}$) in 2 N HCl water solutions (Figure S1), UV−visible spectral changes for the stepwise reoxidations $[Py_8\text{PyzPzMg}(H_2O)]^{2-/1-/0}$ and $[(2\text{-Mepy})_8\text{PyzPzMg}(H_2O)]^{6+/7+/8+}$ (Figure S2 (parts (A,B) and (C,D), respectively)), and UV−visible spectral changes of the stepwise reoxidations $[Py_8\text{PyzPzMg}(H_2O)]^{4-/3-/2-}$ and the parallel reoxidations $[(2\text{-Mepy})_8\text{PyzPzMg}(H_2O)]^{4+/5+/6+}$ (Figure S3 (parts (A,B) and (C,D), respectively)). This material is available free of charge via the Internet at http://pubs.acs.org.

IC051085D